Space Object Classification using Fused Features of Time Series Data

Bin Jia
Intelligent Fusion Technology Inc., Germantown, MD.
Khanh D. Pham
Air Force Research Lab, Kirtland AFB, NM.
Erik Blasch
Air Force Research Lab, Arlington, VA.
Dan Shen, Zhonghai Wang, Genshe Chen
Intelligent Fusion Technology Inc., Germantown, MD.

ABSTRACT

In this paper, a fused feature vector consisting of raw time series and texture feature information is proposed for space object classification. The time series data includes historical orbit trajectories and asteroid light curves. The texture feature is derived from recurrence plots using Gabor filters for both unsupervised learning and supervised learning algorithms. The simulation results show that the classification algorithms using the fused feature vector achieve better performance than those using raw time series or texture features only.

1. INTRODUCTION

The space environment has become congested due to the increasing number of man-made space objects and space debris. Monitoring resident space objects (RSOs) is urgent due to the increasing complexity caused by the interaction of different space objects within the space environment. Many of these RSOs provide support for communications, navigation, and terrestrial analysis. Space situational awareness (SSA) has been intensively investigated [1-6]. Many problems, such as space object tracking, sensor management, conjunction analysis, and uncertainty propagation, are interrelated and intensively studied [7-9]. However, space object recognition or classification is still a challenging problem due to limited sensor resources [10]. Although RSO historical data is available, it is often discarded without further investigation. This paper uses the historical time series data, i.e., historical orbit trajectories and asteroid light curves, to classify space objects.

Object assessment, or Level 1 information fusion in the Data Fusion Information Group (DFIG) model [11], includes object detection, recognition, classification, and identification. Many methods are available such as the recent trends in machine learning and machine analytics [12]; but there is limited data for RSO analysis. Zhang *et al*., provides an example of RSO classification using hyperspectral data [13] and Payne *et al*., [14] uses illumination signatures for RSO classification. Many classification algorithms can be applied, such as the hierarchical clustering for the unsupervised learning and support vector machine (SVM) for the supervised learning. For both kinds of learning algorithms, a data sequence can be directly used for classification. When the length of the time series data is long, the dimension reduction algorithms can be performed [15-18] such as the down-sampling method [15]. Other methods using approximating straight lines [17] or by preserving the salient points [18] are also available. Besides directly using the raw or sampled data sequence in the time domain as the feature vector in the learning algorithms; the representation in a transformed domain could also be used, such as the discrete Fourier transformation (DFT) [19] and the discrete wavelet transformation (DWT) [20].

When the features of the time series data are available, distance or similarity measures are used to evaluate time series classification algorithms. The similarity measures can be roughly categorized as the whole sequence matching or subsequence matching. For the *whole sequence matching*, the most popular approach is to evaluate the Euclidean distance between two time series based on the transformed representations, such as using the DFT/DWT coefficients [20, 22]. However, the Euclidean distance is not always a suitable distance measure and the dynamic time warping (DTW) technique [21] is often used in applications. Based on various distances and similarity measures, further classification, indexing, motif discovery can be processed, where more details can be found in [23]. For *sub-sequence matching*, the time series data is divided into intervals from which patterns are compared to known

exemplars. Sub-sequence methods can be aligned with whole-sequence matching methods based on the selected intervals of observation.

This paper investigates space object classification using the fused feature vector of energy and light curve time series data. Although only the historical orbit data and light curves are used, different time series can be directly applied and integrated into the data fusion method for object classification. Other contextual data [24] would also enhance RSO classification such as the space environment and sun illumination, that benefit from recent efforts in developing a space ontology classification taxonomy [25, 26].

The remainder of the paper is organized as follows. Section II introduces the data preprocessing. Section III introduces the recurrence plot, Gabor features, and the similarity metric. Simulations and numerical results are described in Section IV. Section V gives the concluding remarks.

2. DATA PREPROCESSING

For resident space object classification, various sources of data could be used for the analysis. In this paper, two different kinds of data set are used for object classification. The first data set is the *historical satellite orbit data* and the second data set is the *light curve data of asteroids*.

Historical satellite orbit data

To explore patterns and clustering of different space objects, 141 trajectories were assembled that correspond to different resident space object (RSO) orbits. All trajectories are obtained from the North American Aerospace Defense Command (NORAD) celestrak database [27], which collects orbit data from 1980 to 2004 in two-line elements (TLEs). The length of the historical trajectories varies from a hundred points to thousands of points. For a fair comparison during training, all the trajectories were tailored to the same length. The orbit data (variables) extracted from the two-line element (TLE) includes inclination, eccentricity, argument of perigee, mean anomaly, right ascension of ascending node, and mean motion. The time series data corresponding to each variable can be used to analysis the behavior and classify space objects. For convenience, the energy is used to represent the status of the space object since the energy change effectively represents the change the maneuvers, collisions, and atmospheric density change [28].

The energy per unit mass can be computed by [28]

$$E = -0.5\left(\frac{\pi n G M}{43200}\right)^{\frac{2}{3}} \tag{1}$$

where n denotes the mean motion of the space object, G is the universal gravitational constant, and M is the mass of the Earth.

Before classifying space objects based only on the energy time series data, it is better to explore the performance analysis of the classification method against the available data. For convenience, 141 trajectories were labeled into 27 classes. The data sequence number of some classes is very small, as shown in Figure 1. In order to test the fused feature based classification method, three classes with moderate numbers of data sequences were selected.

Light curve data of asteroids

Light curves have been used in space object classification [14]. Specifically, a physics-based model is often used to connect the light curve observation and the physical properties of the space object. For example, the *Ashikhmin-Shirley model* is often used to produce the light curve of the space object when the parameters of the space object are given, such as the shape and attitude [29]. Although the physical model can be used in some cases, it is generally not a practical method for large scale RSO assessment. First, the model-based method is computationally expensive when the number of space objects is large. Second, the parameters of the space objects are often unknown. Hence, in this paper, rather than using the synthetic data of a physical model with assumed parameters, real data are acquired from public databases. The light curve data is obtained from the asteroid light curve database [30]. There are many

asteroids where light curves exist, but the classification of these RSOs was not done systematically. Thus, it is very helpful to identify their spectroscopic class in order to perform spectroscopic investigation.

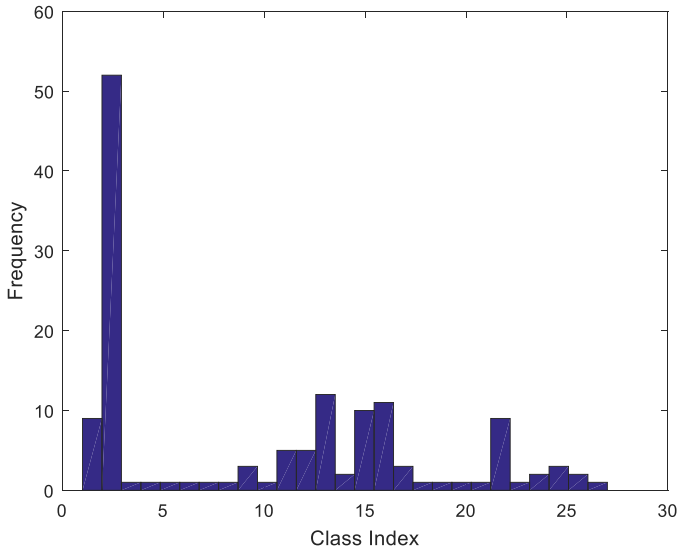

Fig. 1. Frequency of different classes.

Although the light curve database [30] includes many observations of minor planets, the observation periods for many of the space objects are too short to give a complete light curve. Hence, in this paper, only the longest set of observations for each individual object is considered. In addition, the length of the observations was organized into 150 observations. Note that the data was combined from different asteroids with different rotation periods and classes. To prepare the dataset, we use the open source code and tools in [31]. Finally, space objects with two different classes are considered. The light curve data use in the study are shown in Figure 2. Note that the asteroid light curves corresponding to different types are shown in different colors. From Figure 2, it is hard to classify the RSOs by the light curve magnitude only.

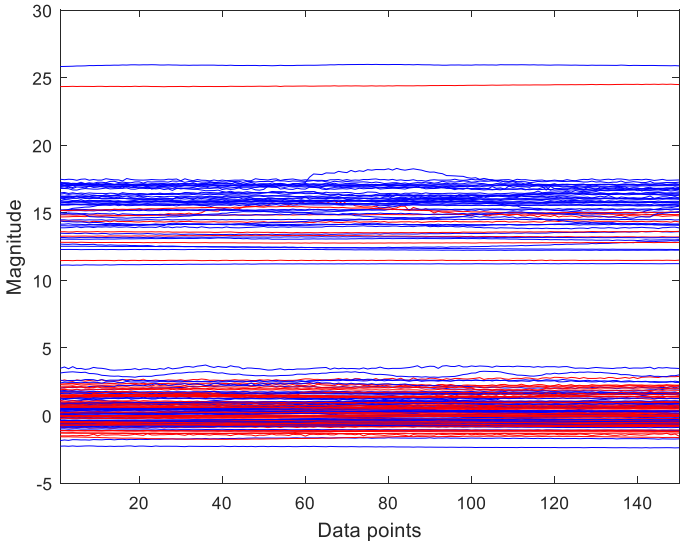

Fig. 2. The magnitude of asteroid light curve

3. FEATURE EXTRACTION AND SIMILARITY DESCRIPTION

As mentioned in Section 1, features can be extracted and the similarity between different data sequences can be derived. The simplest way is to use all data points or sampled data points from the data sequence to form the feature vector. The Euclidean distance is then used as the distance or similarity evaluation metric. For convenience, this straightforward method will be referred to Method-I: *data features*.

The feature vector using all data points in the data sequence often fails to capture the essential structure or motif of the data sequence, which causes the low accuracy of the classification. Fusing texture feature of the data sequence is proposed to enhance the RSO classification. For some time series, which don't have representative features in the time domain, the texture feature can used to solve the classification problem [20]. To extract the texture feature, first, one obtains the recurrence plots (RP). The recurrence plot is given by

$$R_{i,j} = \Theta\left(\varepsilon - \left\|\vec{x}_i - \vec{x}_j\right\|\right), \quad i, j = 1, \cdots, N \tag{2}$$

where N is the number of data points. i and j are indexes. ε is the threshold for closeness. $\Theta(\cdot)$ is the Heaviside step function. Note that the recurrence plot obtained by Eq. (2) is a binary image. The threshold in real applications is hard to choose. In addition, the binary image is lossy as some information fidelity between 0 and 1 is discarded. To improve upon the binary image, the threshold is removed.

The texture is extracted from recurrence plot as a feature. There are many different texture descriptors, such as Local Binary Pattern [32-35], Gray Level Co-occurrence Matrix [36], Gabor filters [37], and Segmentation-based Fractal Texture Analysis [26]. In this paper, we use the Gabor filters to extract texture feature from the recurrence plot.

The image obtained via the recurrence plot is first convolved by a Gabor Wavelet Transform using a set of Gabor filters. Note that the Gabor filters extract different orientations and spatial frequencies. The output of the convolution at a pixel is the information about the spatial relationship between the pixel to its neighbors. The texture features are then obtained based on the output recurrence image [37]. The texture feature can be obtained via Gabor filters and the Euclidean distance can be used to classify data sequences. For convenience, Method-II is *texture features*.

Rather than use Method-I and Method-II separately, we propose to integrate them. Specifically, the feature vector includes all data points in the data sequence and the texture feature. The distance between two data sequences d_{ij} is given as

$$d_{ij} = \left\|\mathbf{x}_i - \mathbf{x}_j\right\| + \lambda \left\|\mathbf{v}_i - \mathbf{v}_j\right\| \tag{3}$$

where $\mathbf{x}_i$ and $\mathbf{x}_j$ are the *i*th and *j*th time series. $\mathbf{v}_i$ and $\mathbf{v}_j$ are the texture vector extracted from the *i*th and *j*th time series, respectively. λ is a regulatory parameter. The regulatory parameter is introduced to balance the importance between different features.

Remark: When $\lambda = 0$, the distance or the similarity function degrades to the Euclidean distance. When $\lambda \to \infty$, the similarity function degrades to the texture-vector-based distance.

4. EXPERIMENTS AND PERFORMANCE EVALUATION

Energy trajectory based space object classification

Typical trajectories with different types are shown in Figures 3, 5, and 7. For convenience, we denote them as Type-I, Type-II, and Type-III space objects; respectively. The recurrence plot is shown in Figures 4, 6, and 8; respectively. The patterns shown in recurrence plot are different for different types of trajectories. Hence, the texture feature extracted from the recurrence plot can be used to classify different kinds of space objects. For the Type-I space objects, the energy is decreasing and no active maneuver is shown. For the Type-II space object, the energy is increasing and regular maneuvers can be distinguished. For the Type-III space object, energy is decreasing and the sharp maneuver can be seen. It is summarized in Table I.

Table I. Different types of space objects

Object Type	**Energy**	**Maneuver**
Type I	Decreasing	Not active
Type II	Increasing	Active
Type III	Decreasing	Active

In this section, we use the hierarchical clustering algorithm because the number of classes is not needed to be prespecified.

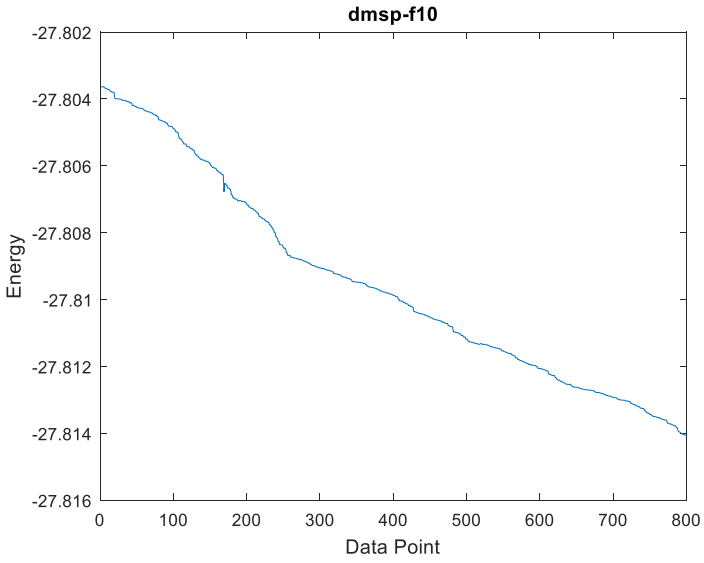

Fig. 3. Typical energy trajectory of Type I space object (dmsp-f10)

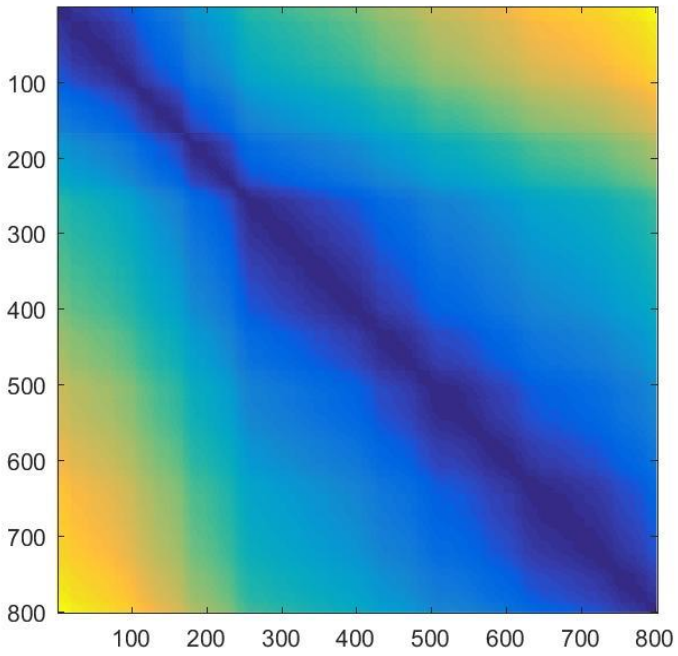

Fig. 4. Recurrence Plot of Type I space object (dmsp-f10)

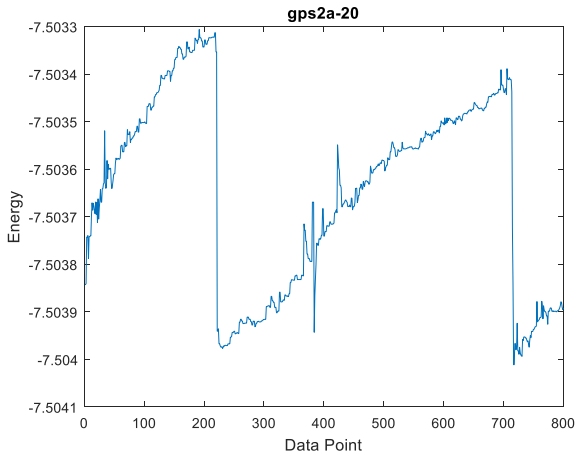

Fig. 5. Typical energy trajectory of Type II space object (gps2a-20)

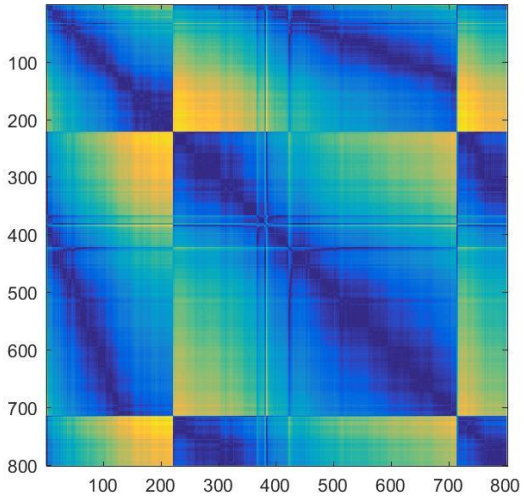

Fig. 6. Recurrence Plot of Type II space object (gps2a-20)

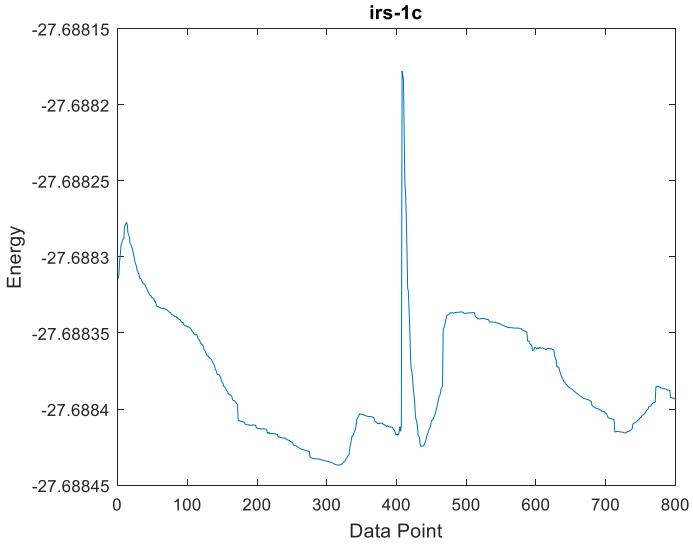

Fig. 7. Typical energy trajectory of Type III space object (irs-1c)

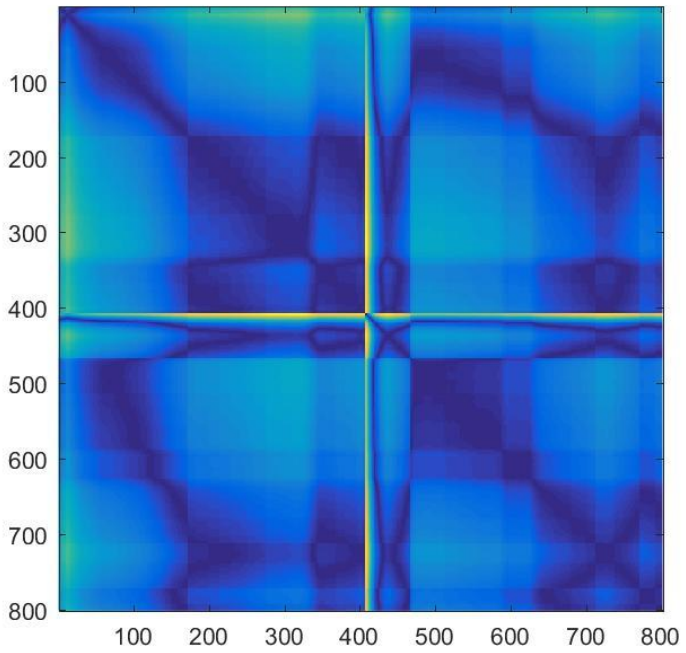

Fig. 8. Recurrence Plot of Type III space object (irs-1c)

The proposed method (Method-III: Integration of data and texture features) is compared to Method-I and Method-II. The dendrogram via the hierarchical clustering algorithm using Method-I (data features) and Method-II (texture features) is shown in Figure 9 and Figure 10, respectively. The dendrogram shows the taxonomic classifications between objects which can be used with an ontology to label RSOs. The dendrogram via the hierarchical clustering algorithm with the Method-III is shown in Figure 11. The accuracy of different methods is given in Table II. It can be seen that Method-III outperforms Method-I and Method II, which shows the benefit of integrating the raw data with the texture feature.

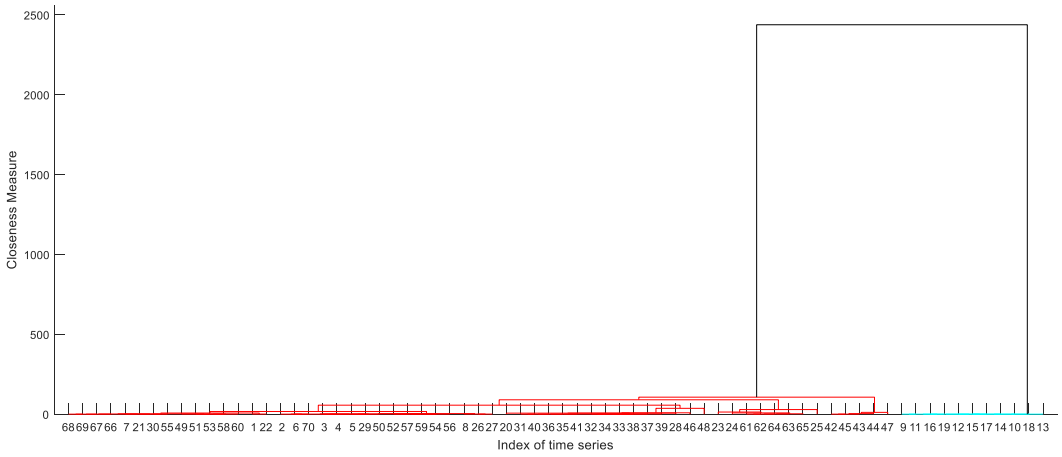

Figure 9. Dendrogram using hierarchical clustering algorithm with the raw data

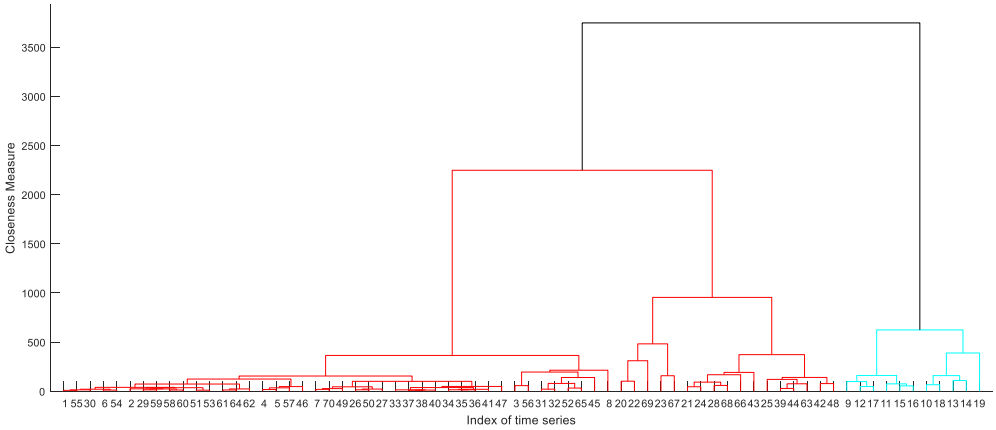

Figure 10. Dendrogram using hierarchical clustering algorithm with the texture feature

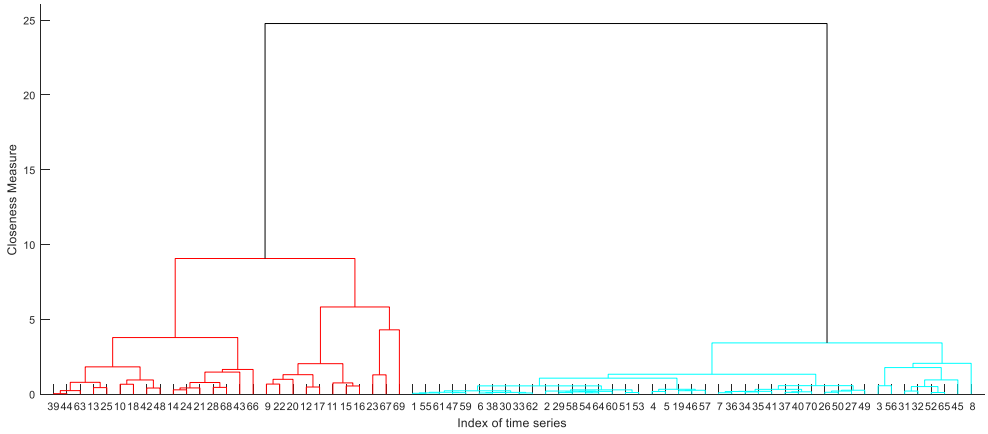

Figure 11. Dendrogram using hierarchical clustering algorithm with the fused feature

Table II, accuracy η of the hierarchical clustering algorithm using different methods

	Method-I	Method-II	Method-III
η	0.8000	0.7429	0.8857

Light Curve based Space Object Classification

To classify asteroids, supervised learning algorithms are used. Specifically, the support vector machine (SVM) algorithm is selected. Typical light curves are shown in Figure 12. It can be seen clearly that the motif of the time sequence is different to each other. As presented in a different form, the recurrence plots for different type asteroid light curves are shown in Figure 13 and Figure 14, respectively. The texture features of Figures 13 and 14 are very different. The Gabor feature mean amplitude for these two images is shown in Figure 15. It can be seen that the texture feature vector for these two types of asteroid light curves are different to each other. Hence, the texture features can be used for the classification algorithm.

To further evaluate the performance of SVM using different features described in Section 3, the receiver operating characteristic (ROC) curves of different methods are shown in Figure 16. As shown in Figure 16, the SVM with fused feature has the best performance. It outperforms both the SVM using texture feature and SVM using only raw data points.

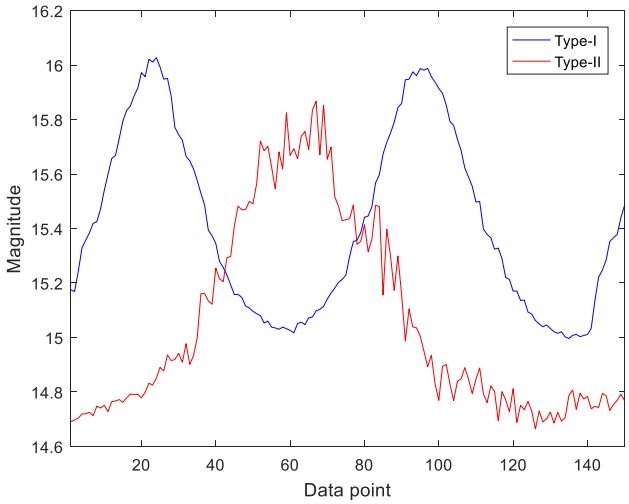

Fig. 12. Two typical asteroid light curve of different types of RSOs

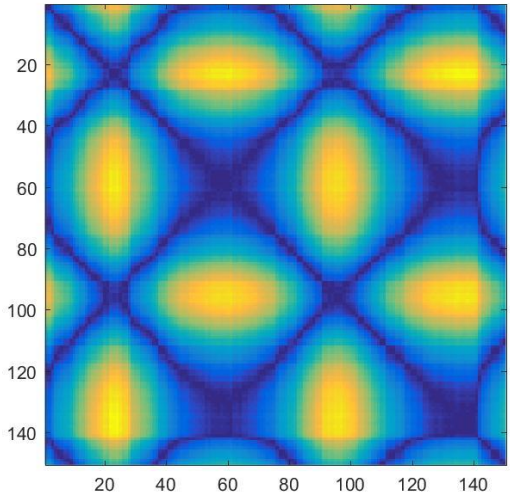

Fig. 13. Recurrence plot for Type-I time sequence in Figure 12

Another investigation question is how to choose the best regulatory parameter, λ. In fact, it can be chosen by the cross-validation procedure. Based on the test results, the performance slightly different when parameter variations are chosen. We select different parameters and use the F-score to evaluate the fused feature SVM performance. The F-score is a relationship between the precision and recall. It can be seen from Figure 17, where the performance using different parameters is close except in cases when the parameters are very small (i.e., close to 0).

5. Conclusion

This paper presents a method for resident space object (RSO) classification based on a fused feature vector. The orbital energy time series and the light curve time series are used to test the performance of fused feature classification methods. The initial results proved effective and revealed that the classification algorithm using the fused feature vector can achieve better performance than the classification algorithm using a single feature vector (e.g., trajectory or light curve) only. Additionally, the regulatory parameter of the fused results did not have a significant impact on the F-score performance evaluation.

Future work would include gathering more contextual information in the analysis, such as space weather, comparing object assessment methods with advanced approaches, and investigating how to optimally chose of the regulatory parameters [38].

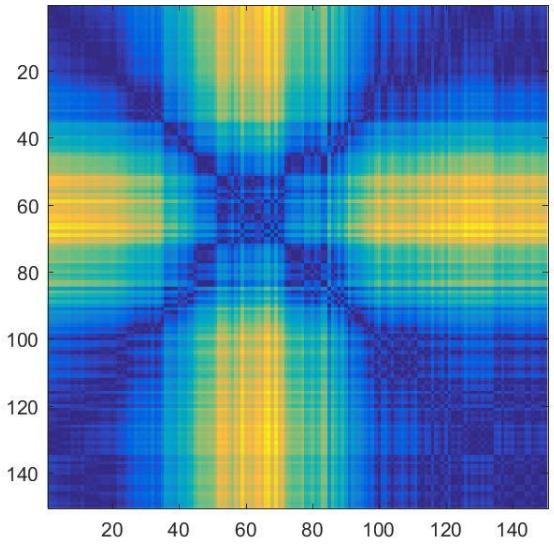

Fig.14. Recurrence plot for Type-II time sequence in Figure 12

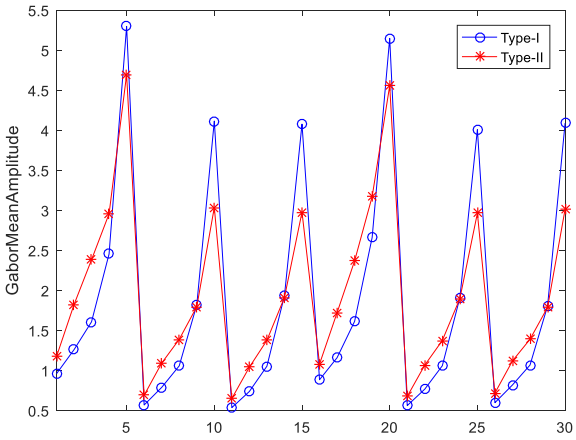

Fig.15. The Gabor Feature Mean Amplitude for different typical asteroid

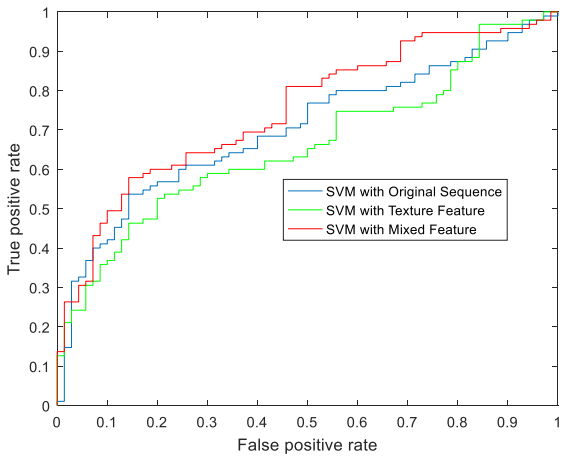

Fig. 16. ROC curves of SVM using different features

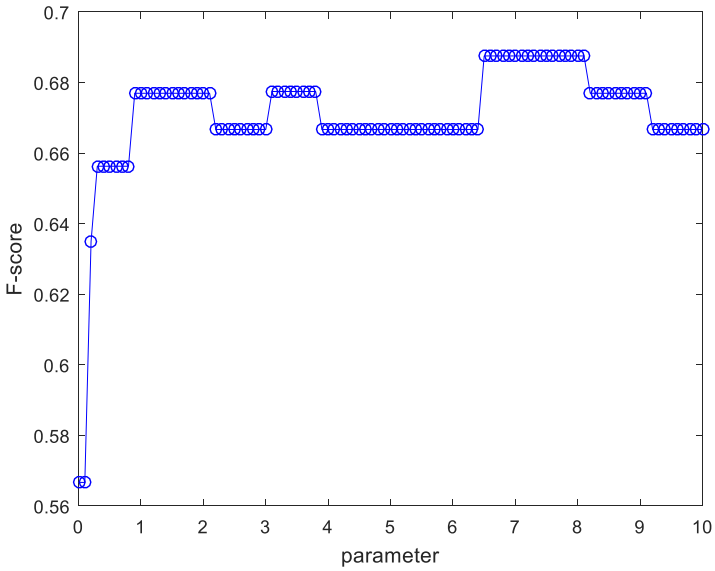

Fig. 17. F-score for SVM using different regulatory parameters.

6. REFERENCES

1. Bobrinsky, N. and Del Monte, L., The space situational awareness program of the European Space Agency, Cosmic Research, vol. 48, no. 5, 392-398, 2010.
2. Blasch, E. P., Pham, K., Shen, D., and Chen, G., Orbital Satellite Pursuit-Evasion Game-Theoretical Control, IEEE Int'l. Conf. on Info. Sci., Sig. Processing and App. (ISSPA), 2012.
3. Shen, D., Chen, G., Pham, K., and Blasch, E., A Trust-based Sensor Allocation Algorithm in Cooperative Space Search Problems, Proc. SPIE, vol. 8044, 2011.
4. Jia, B., Blasch, E., Pham, K. D., Shen, D., Wang, Z., and Chen, G., Cooperative space object tracking via multiple space-based visible sensors with communication loss, IEEE Aerospace Conference, 2014.
5. Jia, B., Pham, K. D., Blasch, E., Shen, D., Wang, Z., and Chen, G., Cooperative space object tracking using consensus-based filters, International Conference on Information Fusion, 2014.
6. Jia, B., Pham, K. D., Blasch, E., Shen, D., Wang, Z., and Chen, G., Cooperative Space Object Tracking using Space-based Optical Sensors via Consensus-based Filters, IEEE Transactions on Aerospace and Electronics Systems, Vol. 52, No. 3, 1908-1936, 2016.
7. Shen, D., Jia, B., Chen, G., Pham, K., and Blasch, E., Game optimal sensor management strategies for tracking elusive space objects, Aerospace Conference, 2017.
8. Jia, B., Pham, K.D., Blasch, E., Shen, D., and Chen, G., Consensus-based auction algorithm for distributed sensor management in space object tracking, Aerospace Conference, 2017.
9. Jia, B., Cai, S., Cheng, Y., and Xin, M., Stochastic collocation method for uncertainty propagation, AIAA/AAS Astrodynamics Specialist Conference, Minneapolis, Minnesota, 2012.
10. Oliva, R., Blasch, E., Ogan, R., Applying Aerospace Technologies to Current Issues Using Systems Engineering, 3rd AESS Chapter Summit, IEEE Aerospace and Electronic Systems Magazine, Vol. 28, No. 2, Feb. 2013.
11. Blasch, E., Lambert, D. A., Valin, P., . Kokar, M. M, Llinas, J., Das, S., Chong, C-Y., and Shahbazian, E., High Level Information Fusion (HLIF): Survey of Models, Issues, and Grand Challenges, IEEE Aerospace and Electronic Systems Mag., Vol. 27, No. 9, Sept. 2012.
12. Blasch, E., Steinberg, A., Das, S., Llinas, J., Chong, C.-Y., Kessler, O., Waltz, E., and White, F., Revisiting the JDL model for information Exploitation, Int'l Conf. on Info Fusion, 2013.
13. Zhang, Q., Wang, H., Plemmons, R. J., and Pauca, V. P., Tensor methods for Hyperspectral Data Analysis: A Space Object Material Identification Study, J. Optical Society of America, A, vol. 25, 3001-3012, 2008.
14. Payne, T., Chaudhary, A., Gregory, S., Brown, J., and Nosek, M., Signature Intensity Derivative and its Application to Resident Space Object Typing, Adv. Maui Optical and Space Surveillance Tech. Conf., 2009.

15. Astrom, K.J., On the choice of sampling rates in parametric identification of time series, Information Sciences, vol.1, no. 3, 273–278, 1969.
16. Keogh, E. and Pazzani, M., A Simple dimensionality reduction technique for fast similarity search in large time series databases, In: Proceedings of the 4th Pacific-Asia Conference on Knowledge Discovery and Data Mining, 122–133, 2000.
17. Keogh, E., Fast similarity search in the presence of longitudinal scaling in time series databases, In: Proceedings of the Ninth IEEE International Conference on Tools with Artificial Intelligence, 578–584. 1997.
18. Chung, F.L., Fu, T.C., Luk, R., Ng, V., Flexible time series pattern matching based on perceptually important points, In: International Joint Conference on Artificial Intelligence Workshop on Learning from Temporal and Spatial Data, pp. 1–7, 2001.
19. Agrawal, R., Faloutsos, C., and Swami, A., Efficient similarity search in sequence databases, In: Proceedings of the Fourth International Conference on Foundations of Data Organization and Algorithms, 69–84, 1993.
20. Struzik, Z. R. and Siebes, A.P.J.M., Wavelet transform in similarity paradigm, In: Proceedings of the Second Pacific-Asia Conference on Knowledge Discovery and Data Mining, 295–309, 1998.
21. Berndt, D. J. and Clifford, J., "Using dynamic time warping to find patterns in time series," In: AAAI Working Notes of the Knowledge Discovery in Databases Workshop, 359–370, 1994.
22. Chan, K.P., Fu, A., and Yu, C., Haar wavelets for efficient similarity search of time series: with and without time warping, IEEE Transactions on Knowledge and Data Engineering, vol. 15, no. 3, 685–705, 2003.
23. Tak-chung, F., A review on time series data mining. Engineering Applications of Artificial Intelligence, vol. 24, 164-181, 2011.
24. Snidaro, L., Garcia-Herrero, J., Llinas, J., and Blasch, E., (eds.), Context-Enhanced Information Fusion: Boosting Real-World Performance with Domain Knowledge, Springer, 2016.
25. Costa, P. C. G., Laskey, K. B., Blasch, E., and Jousselme, A-L., Towards Unbiased Evaluation of Uncertainty Reasoning: The URREF Ontology, Int. Conf. on Info Fusion, 2012.
26. Cox, A. P., Nebelecky, C. K., Rudnicki, R., Tagliaferri, W. A., Crassidis, J. L., and Smith, B., The Space Object Ontology, International Conference on Information Fusion, 2016.
27. https://www.celestrak.com/NORAD/archives/
28. Patera, R. P., Space event detection method, Journal of Spacecraft and Rockets, vol. 45, no. 3, 554-559, 2008.
29. Lindares, R., Crassidis, J. L., and Jah, M. K. Space object classification and characterization via multiple model adaptive estimation, 17th International Conference on Information Fusion, 1-7, 2014.
30. http://alcdef.org
31. https://2015.spaceappschallenge.org/project/neural-asteroid-classification/
32. Vinicius, M. A. S., Diego, F. S., and Gustavo, E. A. P. A. B., Extracting Texture Features for Time SeriesClassification, 22nd International Conference on Pattern Recognition, 1425-1430, 2014.
33. Doost, H. R. E. and Rahebi, J., An efficient method for texture classification with local binary pattern based on wavelet transformation, IJES, vol. 4, no. 12, 4881–4885, 2012.
34. Ojala, T., Pietikainen, M., and Harwood, D., A comparative study of texture measures with classification based on featured distributions, Pattern Recognition, vol. 29, no. 1, 51–59, 1996.
35. Ojala, T., Pietikainen, M., and Maenpaa, T., Multiresolution gray-scale and rotation invariant texture classification with local binary patterns, IEEE TPAMI, vol. 24, no. 7, 971–987, 2002.
36. Baraldi, A. and Parmiggiani, F., An investigation of the textural characteristics associated with gray level cooccurrence matrix statistical parameters, IEEE TGRS, vol. 33, no. 2, 293–304, 1995.
37. Idrissa, M. and Acheroy, M., Texture classification using gabor filters, Pattern Recognition Letters, vol. 23, no. 9, 1095–1102, 2002.
38. Aved, A., Peng, J., and Blasch, E., Regularized Difference Criterion for Computing Discriminants for Dimensionality Reduction, Accepted to IEEE Trans Aerospace and Electronic Systems, Mar. 2017.